Enhancement of photocatalytic activity of TiO_2 by plasma irradiation

Shin Kajita

*Institute of Materials and Systems for Sustainability, Nagoya University, Nagoya 464-8603, Japan**

Tomoko Yoshida

[3] *The Osaka City University Advanced Research Institute for Natural Science and Technology, Osaka 558-8585, Japan*

Noriyasu Ohno, Tomoya Ishida, Daiki Kitaoka

Graduate School of Engineering, Nagoya University, Nagoya 464-8603, Japan

(Dated:)

Abstract

In this study, plasma irradiations to titanium were conducted to enhance the photocatalytic activity of titanium oxide. When titanium is exposed to He plasmas, various morphology changes occur as forming nano-bubbles near the surface. Photocatalytic activity of the helium plasma irradiated titanium samples with nano-cones and microstructures were assessed by the hydrogen production from aqueous methanol solution. It is shown that the He plasma irradiation increases the photocatalytic activity more than double. Moreover, nitrogen mixture plasma irradiation to titanium (oxide) was conducted for doping nitrogen, which has been regarded as method to create visible light reactivity. It is shown from XPS analysis that nitrogen doping has been successfully conducted under specific conditions.

PACS numbers:

*Electronic address: kajita.shin@nagoya-u.jp

I. INTRODUCTION

Helium (He) plasma irradiation to metals leads to morphology changes and forms various nanostructures on metal surfaces [1–5]. Formation of fiberform nanostructures called 'fuzz' has been first identified on tungsten surface in basic nuclear fusion researches [1], and extensively investigated experimentally [6–9] and theoretically [10, 11] for its potential influences on plasma facing components. To take advantages of the physical and optical property changes, its potential industrial application has been explored as well.

One of the application is for photocatalysis [2, 12–14]. Since hydrogen production from water splitting process by photocatalytic reaction has been identified [15], one of the challenging issues is to develop highly reactive photocatalytic materials with reactivity in visible and/or infrared ranges to use the solar light efficiently [16]. Mesoporus nanostructures have exhibited significantly high catalytic activities [17, 18]. It has been identified that oxides, nitrides, and oxinitrides of some metals including tungsten, tantalum, niobium, and iron have visible light reactivity [19–22]. Also, nitrogen (N) doping is regarded as a way to activate the visible light response on TiO_2 photocatalysis [23, 24]. However, the photocatalytic material with high efficiency to compete electrolysis of water has yet to be developed.

Because the He irradiated nanostructure has an order of magnitude higher surface area [25], totally black photon absorber [26], and highly porous structure in nanometer scale, it is envisaged that the material has a potential to be highly active photocatalytic material. Until now, visible light reactivity has been identified on the He plasma irradiated W partially oxidized [2, 13, 14], and, moreover, it has been shown that the oxidized He plasma irradiated W has higher water splitting efficiency as a photocatalytic material [12]. Therefore, it is of interests to investigate the potential of He plasma irradiation for the development of mesoporus photocatalytic materials. Concerning N doping, although methods using ammonium and urea have been developed, it is not easy to control the amount and depth of doping, and they require additional reagents and special equipment. If the plasma processing can be utilized for N doping, potential of plasma processes as a tool for photocatalytic application will be much broader. The usage of plasma has an advantage in a large area processing short process speed.

In this study, photocatalytic activity of oxidized titanium exposed to a He plasma was investigated using hydrogen production reaction using aqueous methanol solution. Further-

more, we try to inject N atoms on titanium (Ti) using N mixed plasmas. In this study, we focused on the investigation of necessary irradiation conditions for N doping using the plasma. Although the amount of N doping will not be optimized in this study, it is shown that N doping can be properly conducted when irradiation parameters are tuned. This will be an important first step to utilize plasmas for N doping, which can allow the utilization of visible range of solar light. In Sec. II, material tailoring methods including plasma irradiation and oxidization conditions are shown. Sec. III provides results and discussions based on hydrogen production experiments from aqueous methanol solution and of XPS analysis of N mixture plasma irradiated materials.

II. MATERIAL TAILORING

Plasma irradiations were conducted in the linear plasma device NAGDIS-II [27], where high density plasmas can be produced in a steady state. The typical electron density and temperature are, respectively, 10^{19} m^{-3} and <10 eV in NAGDIS-II. He gas was used for the discharge gas, and pure He plasmas without any additional gases were used for He plasma irradiation to induce morphology changes. For N doping experiments, N_2 gas was injected from the downstream of the plasma stream, and the samples were exposed to the N mixed He plasmas.

Table I shows the samples (Ti1-Ti3) used for hydrogen production using aqueous methanol solution. Ti1 is a pristine sample, and Ti2 and Ti3 were titanium samples exposed to the He plasmas under slightly different conditions. All the samples were oxidized in a heating furnace at 773 K for 30 min. For Ti2 and Ti3, the oxidization was conducted after the plasma irradiation. For the photocatalytic experiments, a xenon lamp, which covers wide wavelength range from 300 to infrared, was used for the light source, and produced hydrogen was analyzed using a gas chromatograph. The size of the sample used for the photocatalytic experiments was 10×10 mm^2 with the thickness of 0.3 mm.

Table II shows a summary of the four different samples Ti4-Ti7 for N doping experiments. The sample Ti4 is TiO_2 sample just for reference, Ti5 is a titanium sample irradiated with He-N_2 mixture plasma at the incident energy of 35 eV, Ti6 is a TiO_2 sample irradiated with He-N_2 mixture plasma at the incident energy of 27 eV, and Ti7 is titanium sample irradiated with He-N_2 mixture plasma at the incident energy of 65 eV. Here, the incident energy was

for N, which was calculated from half of the potential difference between the sample and the plasma, because the major N ion should be N_2^+. Concerning the He ion, the incident ion energy should be double that of N ions. For all the irradiation, the fraction of N_2 gas was approximately 45% in the injected amount basis, the surface temperature was ∼600 K during the irradiation, and the total ion fluence was $\sim 10^{25}$ m^{-2}. Oxidization was conducted at 573 K in the air atmosphere using the heating furnace. For Ti5 and Ti7 samples, the oxidization was done after the plasma irradiation.

III. RESULTS AND DISCUSSION

A. Hydrogen production

From previous systematic irradiations [28], it has been found that various structures including nano-cones, microstructures, and fiberform nanostructures are formed by changing the incident ion energy and the surface temperature. Figures 1(a-c) show scanning electron microscope (SEM) micrographs of Ti1, Ti2, and Ti3, respectively. Without plasma irradiation (Ti1), the surface was almost flat without any fine structures. On Ti2, which was exposed to the He plasma at 770 K, nano-cones were formed on the surface, while, on Ti3, which was exposed at 900 K, microstructures were observed. Previously, it has been identified that nano-bubbles were formed inside the structures [2, 28]. In addition to sputtering, which is negligible on tungsten and molybdenum, growth of He bubbles would also play important roles to form nanostructures similar to the morphology changes on other metals during He plasma irradiation [28]. On both of the samples, it is seen that structures formed by the plasma irradiation were sustained even after the oxidization at 770 K. Figure 2 shows XPS spectra around Ti 2p of Ti1-Ti3 after oxidization. Observed two peaks correspond to TiO_2 peaks (Ti-$2p_{3/2}$ and Ti-$2p_{1/2}$) [29], indicating that the surface was sufficiently oxidized on all the samples Ti1-Ti3 after the heating at 773 K. The peak intensity of Ti2 and Ti3 was approximately 30% less than that of Ti1, probably because the density of TiO_2 decreased near the surface by the existence of He bubbles.

Figure 3(a) shows temporal evolutions of hydrogen production from Ti1-Ti3 samples. No optical filter was used for the experiments. On all the samples, produced hydrogen increased with the irradiation time. For three hours, the amounts of hydrogen production

on Ti1, Ti2, and Ti3 were, respectively, 0.8, 0.9, and 1.3 μmol. On He plasma irradiated samples, hydrogen production rate was higher than pristine sample. On Ti3, 60-100% higher amount of hydrogen was produced compared with that on Ti1. From this experiment, it is shown that the He plasma irradiation can improve the efficiency of photocatalytic activity on ethanol decomposition; the possible mechanism will be discussed later.

In recent photocatalytic experiments, TiO_2 nano-particles have been used, and the amount was expressed using a unit of $\mu molg^{-1}h^{-1}$. E.g., on water/methanol decomposition experiments, 17 $\mu molg^{-1}h^{-1}$ hydrogen production on TiO_2 P25 sample was increased by two orders of magnitude by deposition of gold nano-particles [30]. On a $CuO/Al_2O_3/TiO_2$ nanocomposite sample, hydrogen production efficiency was increased approximately ten-fold from pure TiO_2 P25 sample, and was 1×10^3 $\mu molg^{-1}h^{-1}$ of hydrogen was produced from water/methanol solution [31]. Because plate samples were used for experiments in this study, it is difficult to compare the production rate in $\mu molg^{-1}h^{-1}$. In this study, the production rate was 0.44 $\mu molh^{-1}$ from Ti3 with the reaction surface area of 10^{-4} m^2. Considering the fact that the Brunauer-Emmett-Teller (BET) surface area was measured to be 8-56 m^2/g for TiO_2 P25 sample (it varied with the annealing temperature) [32], one can say that the production rate per unit area in this study was not bad.

Next, we installed an optical filter to use only the light with the wavelengths longer than 640 nm. Figure 3(b) shows temporal evolutions of hydrogen production from Ti1-Ti3 samples with the filter. It is seen that hydrogen was produced and the amount of production increased with time on all the samples. Although produced hydrogen was two orders of magnitude less than that in the cases without the filter, significant difference can be identified between the samples. The produced hydrogen was 2-2.5 times greater on Ti2 and Ti3 compared with that on Ti1. Since it is known that hydrogen could not be produced with TiO_2 with photons with less energy than the TiO_2 band gap of 3.2 eV, it is not unclear at the moment why hydrogen production occurred on Ti1 as well. Some impurity on the surface might have worked for the hydrogen production.

Potential factors to increase of the hydrogen production are increases of effective surface area and optical absorbance by the He plasma irradiation. On W samples, increases in the effective surface area measured by BET method was more than 10 fold when fuzzy nanostructures were formed on the surface [25]. Although the increase in the effective surface area may be less significant compared with W cases, because the morphology changes were

simpler on Ti, the effective surface area could be increased by several times on titanium by the He plasma irradiation. The BET measurement of the surface area is not easy for the sample used, because the effective surface area is comparable to that of test tube. Concerning nano-cone surfaces, the effective surface area is determined from the density of the nano-cones and the aspect ratio of cones. Curved surface area of a cone can be written with the radius, r, and the height, h, as

$$\pi r\sqrt{h^2 + r^2}. \tag{1}$$

Assuming that h/r is $\sim$5 and the filling factor of cones is 0.5 using examples from the previous observation [28], it is assessed that the surface area is increased by a factor of $\sim$3. On Ti3, on which microstructures were formed, the actual area is at the moment unknown. Although the increase of the surface area would be much less than fuzzy surface, considering the fact that Ti3 had better photocatalytic activity, the surface area of Ti3 could be greater than that of Ti2.

Figure 4 shows wavelength dependences of the optical reflectance of Ti1 and He plasma irradiated TiO_2 sample with microstructures (similar to Ti3). Here, because the sample was not in powder form but was plate, the photon absorption does not necessary correspond to electronic excitations. It is seen that the optical reflectance of the He plasma irradiated sample is lower than Ti1 from ultraviolet to visible wavelength range. The optical reflectance of the He irradiated TiO_2 is approximately 30% lower than Ti1. The increases in the surface area and the optical absorbance would play an important role to improve the efficiency.

It is of interest to note that increase of photocatalytic activity by the plasma irradiation was greater when the filter was used. It is at the moment not clear whether visible light responsiveness was caused by the plasma irradiation, because it was also identified on the sample without plasma irradiation. At the moment, the processes and the mechanism are not clear, and we cannot exclude the possibility that impurities existed on all the samples might have reacted with visible light. However, the results suggested that the He plasma irradiation could enhance the photocatalytic activity especially in longer wavelength range on titanium surfaces. On plasma irradiated partially oxidized W sample (WO_3/W composite), decolorization of methylene blue was induced by near infrared light irradiation [13], and later verified that decomposition of methylene blue was really proceeded by the near infrared light irradiation from detailed sulfur K-edge XANES measurement [14]. It was suggested that

photoexcitation by surface plasmon resonance on the nanosized W followed by electron injection into the conduction band of nanosized WO_3 surface at WO_3/W interface resulted in the reaction with methylene blue molecules [13]. Enhancement of photocatalytic activity shown in Fig. 3(b) might be induced in the manner similar to WO_3/W composite case.

B. N doping

To characterize the chemical state of the implanted N on samples, XPS measurement was conducted after the irradiation. Figure 5(a) and (b) shows XPS spectra for Ti4-Ti7 around N 1s and Ti 2p peaks, respectively. Concerning N 1s spectra, the peak at 397 eV can be attributed to titanium nitride [29], while the one at 396 eV can be assigned to nitrogen substituting O sites of TiO_2 [33], which was identified photocatalytically active nitrogen doped TiO_2. For the peak around Ti 2p, we can identify amorphous TiO_2 peaks (Ti-$2p_{3/2}$: 458 eV, Ti-$2p_{1/2}$: 464 eV) and TiN peaks (Ti-$2p_{3/2}$ 455 eV, Ti-$2p_{1/2}$: 461 eV) [29].

On Ti4, clear TiO_2 peaks at 458 and 464 eV were identified without any N 1s peaks around 397 eV. On Ti5, peaks at 397 and 396 eV were identified in Fig. 5(a), suggesting that N was properly injected on titanium by the exposure to the N mixture plasma. However, after oxidization, the N 1s spectra totally disappeared, indicating that the injected N atoms were released from the surface during the oxidization. For Ti6, the N 1s spectra was also identified even after the plasma irradiation, indicating that N injection is possible for TiO_2 as well. However, from Ti 2p spectra in Fig. 5(b), it was identified that TiN peak was greater than TiO_2 peak, suggesting that TiO_2 layer was removed almost totally. When plasma irradiation was conducted at higher energy of 65 eV (Ti7), N 1s peak was identified even after the oxidization. In addition, TiO_2 peak was much greater than that of TiN after oxidization. The peak at 396 eV identified on oxidized Ti7 indicates that N substituted the O site of TiO_2.

The threshold energy of N atom for displacement of titanium atom is calculated to be $\sim$47 eV with using the average displacement energy of 30 eV [34]. Thus, different from Ti4, the incident energy of which was lower than the threshold energy, displacement of titanium atoms can easily occur by N atom bombardment on Ti6, where the incident energy was higher than the threshold energy. It can be said that N atoms can be remained even after oxidization when significant displacement occurs. On the other hand, it was suggested that

N atoms existed interstitially on Ti5 and were released during the oxidization process.

Considering the practical application of plasma irradiations for Ti, a combination of the usages of He plasma irradiation for morphology changes and N irradiation for N doping, followed by the oxidization is the plausible processes. It is expected that photocatalytic activity is enhanced by the morphology changes. In the present study, it was confirmed that the N-doping is possible with using N mixture plasmas when increasing the incident ion energy of N to 65 eV. It is expected that the N-doping can expand active wavelength ranges and develop visible light responsive photocatalyst. For practical application, further experiments are required to optimize the amount of doped N and to find appropriate reactions with which the effect of doped N can be clearly identified; they are the issues for future work.

IV. CONCLUSIONS

Photocatalytic hydrogen production from aqueous methanol solution was performed with oxidized helium (He) plasma irradiated nanostructured titanium. When titanium samples were irradiated to the helium plasmas, nano-cones and microstructures were formed on the surface. The titanium samples were oxidized at 773 K for 30 min and photocatalytic activity was investigated. The helium plasma irradiated samples had higher photocatalytic activity, and the hydrogen production rate was increased by 100-150% especially when the visible light ($>$ 640 nm) was used for photon source. Moreover, nitrogen (N) doped TiO_2 was fabricated by N-He mixture plasma irradiation. It was found that the incident energy was important factor to sustain the injected N on titanium after oxidation. When the incident energy was 65 eV, N atoms were remained on the surface even after oxidization at 573 K, while at 35 eV, N atoms disappeared from the surface during the oxidization even though N was injected. From the XPS spectral analysis, it was found that photocatalytically active N substituting O site of TiO_2 was formed on the surface.

Acknowledgements

This work was supported in part by a Grant-in-Aid for Scientific Research (B) 15H04229 and a Grant-in-Aid for Exploratory Research 16K13917 from the Japan Society for the

Promotion of Science (JSPS) and NIFS collaborative research program (NIFS15KOAH032).

[1] S. Takamura, N. Ohno, D. Nishijima, and S. Kajita: Plasma Fusion Research **1** (2006) 051.

[2] S. Kajita, T. Yoshida, D. Kitaoka, R. Etoh, M. Yajima, N. Ohno, H. Yoshida, N. Yoshida and Y. Terao: Journal of Applied Physics **113** (2013) 134301.

[3] I. Tanyeli, L. Marot, M. C. M. van de Sanden and G. De Temmerman: ACS Applied Materials & Interfaces **6** (2014) 3462.

[4] S. Takamura and Y. Uesugi: Applied Surface Science **356** (2015) 888 .

[5] S. Kajita, T. Ishida, H. Dogyun, N. Ohno and T. Yoshida: Sci. Rep. **6** (2016) 30380.

[6] M. Baldwin and R. Doerner: Nucl. Fusion **48** (2008) 035001 (5pp).

[7] S. Kajita, S. Takamura and N. Ohno: Nucl. Fusion **49** (2009) 032002.

[8] G. De Temmerman, K. Bystrov, J. J. Zielinski, M. Balden, G. Matern, C. Arnas and L. Marot: Journal of Vacuum Science & Technology A **30** (2012) 041306.

[9] Y. Ueda, H. Peng, H. Lee, N. Ohno, S. Kajita, N. Yoshida, R. Doerner, G. D. Temmerman, V. Alimov and G. Wright: Journal of Nuclear Materials **442** (2013) S267 .

[10] S. I. Krasheninnikov: Physica Scripta **2011** (2011) 014040.

[11] A. Ito *et al.*: Nuclear Fusion **55** (2015) 073013.

[12] M. de Respinis, G. De Temmerman, I. Tanyeli, M. C. van de Sanden, R. P. Doerner, M. J. Baldwin and R. van de Krol: ACS Applied Materials & Interfaces **5** (2013) 7621.

[13] K. Komori, T. Yoshida, S. Yagi, H. Yoshida, M. Yajima, S. Kajita and N. Ohno: e-J. Surf. Sci. Nanotech. **12** (2014) 343.

[14] K. Komori, T. Yoshida, T. Nomoto, M. Yamamoto, C. Tsukada, S. Yagi, M. Yajima, S. Kajita and N. Ohno: Nuclear Instruments and Methods in Physics Research Section B: Beam Interactions with Materials and Atoms **365, Part A** (2015) 35 .

[15] A. Fujishima and K. Honda: Nature **238** (1972) 37.

[16] X. Chen, S. Shen, L. Guo and S. S. Mao: Chemical Reviews **110** (2010) 6503, pMID: 21062099.

[17] D. R. Rolison: Science **299** (2003) 1698.

[18] X. Chen, T. Yu, X. Fan, H. Zhang, Z. Li, J. Ye and Z. Zou: Applied Surface Science **253** (2007) 8500 .

[19] Z.-G. Zhao and M. Miyauchi: Angewandte Chemie International Edition **47** (2008) 7051.

[20] M. Seki, H. Yamahara and H. Tabata: Applied Physics Express **5** (2012) 115801.

[21] G. Hitoki, T. Takata, J. N. Kondo, M. Hara, H. Kobayashi and K. Domen: Chem. Commun. **16** (2002) 1698.

[22] T. Takata, G. Hitoki, J. N. Kondo, M. Hara, H. Kobayashi and K. Domen: Research on Chemical Intermediates **33** (2007) 13.

[23] R. Asahi, T. Morikawa, T. Ohwaki, K. Aoki and Y. Taga: Science **293** (2001) 269.

[24] H. Irie, Y. Watanabe and K. Hashimoto: The Journal of Physical Chemistry B **107** (2003) 5483.

[25] M. Yajima, Y. Hatano, S. Kajita, J. Shi, M. Hara and N. Ohno: Journal of Nuclear Materials **438** (2013) S1142.

[26] S. Kajita, T. Saeki, N. Yoshida, N. Ohno and A. Iwamae: Applied Physics Express **3** (2010) 085204.

[27] S. Takamura, N. Ohno, D. Nishijima and Y. Uesugi: Plasma Sources Sci. Technol. **11** (2002) A42.

[28] S. Kajita, D. Kitaoka, N. Ohno, R. Yoshihara, N. Yoshida and T. Yoshida: Applied Surface Science **303** (2014) 438 .

[29] F.-H. Lu and H.-Y. Chen: Thin Solid Films **355-356** (1999) 374 .

[30] S. Oros-Ruiz, R. Zanella, R. Lopez, A. Hernandez-Gordillo and R. Gomez: Journal of Hazardous Materials **263, Part 1** (2013) 2 .

[31] T. Miwa, S. Kaneco, H. Katsumata, T. Suzuki, K. Ohta, S. C. Verma and K. Sugihara: International Journal of Hydrogen Energy **35** (2010) 6554 , iSMF-09International Symposium on Multiphase Flow, Heat Mass Transfer and Energy Conversion.

[32] K. J. A. Raj and B. Viswanathan: Indian Journal of Chemistry **48A** (2009) 1378.

[33] T. Yoshida, S. Niimi, M. Yamamoto, T. Nomoto and S. Yagi: Journal of Colloid and Interface Science **447** (2015) 278 .

[34] M. Nastasi, J. Mayer and J. K. Hirvonen, *Ion-Solid Interactions: Fundamentals and Applications* (Cambridge University Press, 2004).

TABLE I: Samples used for hydrogen production from aqueous methanol solution.

Sample No	Incident ion energy	Surface temperature	He fluence
Ti1	n/a	n/a	n/a
Ti2	78 eV	770 K	5.3×10^{25} m^{-2}
Ti3	83 eV	900 K	2.4×10^{25} m^{-2}

TABLE II: A summary of the samples used for nitrogen doping. Oxidization (Oxid.) was conducted on Ti4 samples, while plasma irradiation (Plasma irrad.) and oxidization were conducted on Ti5-7 samples.

Sample No	Processes	Plasma irradiation
Ti4	Oxid.	n/a
Ti5	Plasma irrad. $\rightarrow$ Oxid.	He-N_2 plasma at 35 eV
Ti6	Oxid. $\rightarrow$ Plasma irrad.	He-N_2 plasma at 27 eV
Ti7	Plasma irrad. $\rightarrow$ Oxid.	He-N_2 plasma at 65 eV

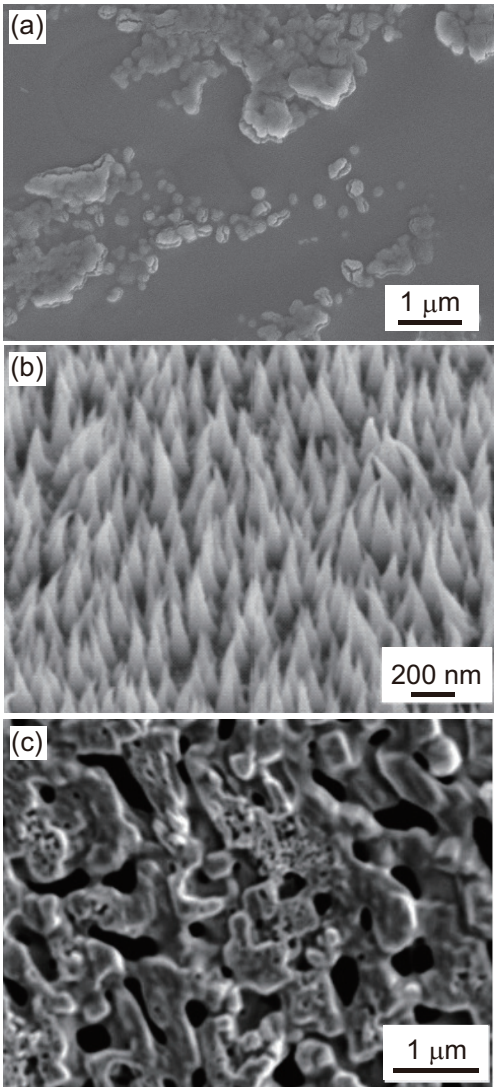

FIG. 1: SEM micrographs of (a) Ti1, (b) Ti2, and (b) Ti3.

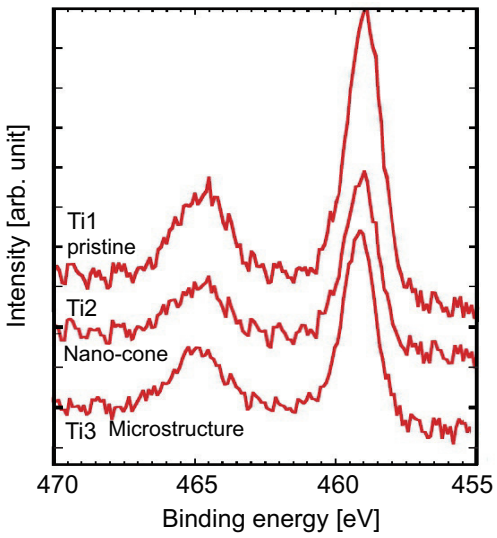

FIG. 2: XPS spectra around Ti 2p of Ti1-Ti3 after oxidization.

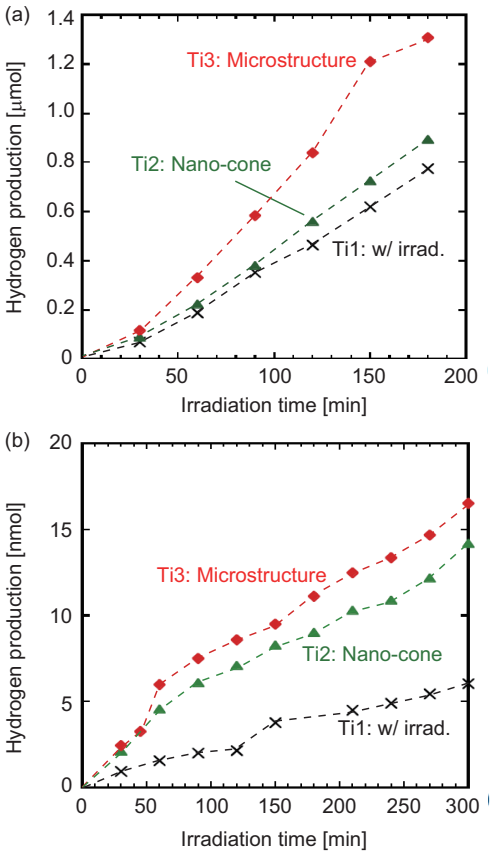

FIG. 3: Temporal evolutions of hydrogen production from Ti1-Ti3 samples (a) without and (b) with an optical filter.

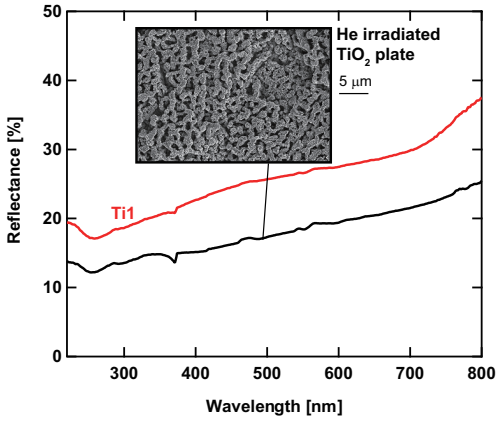

FIG. 4: Wavelength dependence of the optical reflectance of Ti1 and He plasma irradiated TiO_2 sample with microstructures (similar to Ti3).

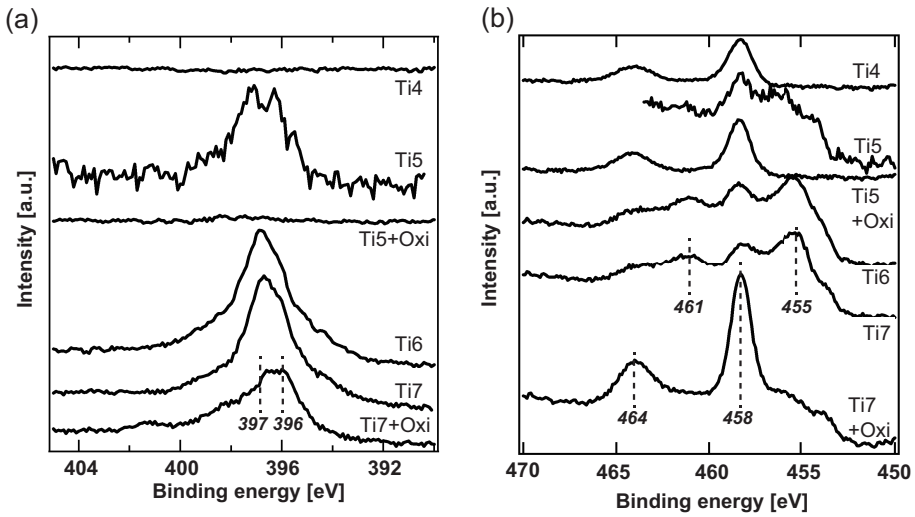

FIG. 5: XPS spectra of Ti4-Ti7 samples around (a) N 1s and (b) Ti 2p peaks. (On Ti5 without oxidization, different XPS device was used and the scale of the intensity was different than the others.)